http://dx.doi.org/10.5935/0103-5053.20130130
J. Braz. Chem. Soc., Vol. 24, No. 6, 1012-1017, 2013.
Printed in Brazil - ©2013 Sociedade Brasileira de Química
0103 - 5053 $6.00+0.00

Article

Morphology of Soy Protein Isolate at Oil/Water and Oil/Air Interfaces

Samira J. Fayad,[a] Betina G. Zanetti-Ramos,[b] Pedro L. M. Barreto,[c] Valdir Soldi[a] and Edson Minatti*[,a]

[a]*Departamento de Química, Universidade Federal de Santa Catarina, 88040-900 Florianópolis-SC, Brazil*

[b]*Departamento de Ciências Farmacêuticas, Universidade Federal de Santa Catarina, 88040-970 Florianópolis-SC, Brazil*

[c]*Departamento de Ciência e Tecnologia de Alimentos, Universidade Federal de Santa Catarina, 88034-001 Florianópolis-SC, Brazil*

Neste artigo, as propriedades emulsificantes da proteína isolada de soja (SPI) foram evidenciadas mostrando que estas macromoléculas sofrem mudanças conformacionais quando adsorvidas em interfaces. Investigou-se a conformação das cadeias proteicas ancoradas nas regiões interfaciais de emulsões de óleo em água (o/a) através de técnicas de espalhamento de raios X (SAXS) e de imagem (microscopia eletrônica de varredura (SEM)). O valor médio do raio de giro (R_g) da SPI (aq) é 20 nm e aumenta para 30 nm em emulsões o/a; as proteínas atuam como moléculas anfifílicas expondo seus núcleos hidrofóbicos ao óleo e os resíduos hidrofílicos à fase aquosa. Este valor ainda é maior após o *spray drying* das emulsões, na interface o/ar das respectivas microcápsulas. As paredes das microcápsulas são fractais de objetos agregados com superfícies rugosas, que são alisadas pela presença de um agente de reticulação.

Herein, the emulsifying properties of soy protein isolate (SPI) were highlighted by showing that the macromolecules undergo conformational changes when adsorbed at interfaces. The conformation of protein chains nested at the interfacial region of oil in water (o/w) emulsions by means of X-ray scattering (SAXS) and direct imaging (scanning electron microscopy (SEM)) techniques was investigated. The mean radius of gyration (R_g) for SPI (aq) is 20 nm and increases up to 30 nm in o/w emulsions; the proteins act as amphiphilic molecules by exposing their hydrophobic core to the oil and their hydrophilic amino acid residues to the water phase. By spray drying the emulsions, it was also possible to measure the size (R_g = 40 nm) and to evaluate the morphology of these proteins at the oil/air interface of the respective microcapsules. The walls of microcapsules are fractals of clustered objects with rough surfaces, which are smoothed by the presence of a cross-linking agent.

Keywords: interface, emulsion, protein, surface, microcapsules

Introduction

The benefits of using biopolymers as emulsifiers are several; for instance, they are usually cheaper than synthetic polymers, natural polymers are more environmentally friendly (biocompatible and biodegradable) and they can usually be obtained through simple extraction/precipitation techniques, with no need for hard chemistry or organic solvents. The fact that Brazil is one of the top world producers of soybean is another motivation for the development of new products based on the biopolymers that can be obtained from this product.[1]

One of the peptide fractions of the dried extract of soybeans is known as soy protein isolate (SPI), which is a mixture of several different proteins, in which the major constituents are globulins.[2] These globular proteins may self-associate to form spherical aggregates in water and the resulting system is an aqueous suspension of these aggregates.[3]

The emulsifying properties of SPI are already known and it has been found to be a very good foam stabilizer.[2,4] Some studies have shown the possibility of producing microcapsules of SPI, obtained either by spray drying emulsions or by coacervation methods.[5-10] The cysteine residues in the protein backbone allow cross-linking of the polypeptide chains by simply heating,

*e-mail: edson.minatti@ufsc.br

with no need for cross-linking agents due to the formation of inter and intramolecular disulfide bridges.[11]

This research forms part of a strategy to encapsulate the oil from the Copaiba tree, which has been used as an anti-inflammatory and anti-septic and has shown activity against the parasite *Leishmania amazonensis*.[12,13] In this study, oil in water (o/w) emulsions using SPI as the emulsifier were prepared and from the obtained samples microcapsules of SPI with oil were prepared through spray drying the emulsions. Herein, the emulsifying properties of SPI and the morphological changes that SPI undergoes when nested at oil/water and oil/air interfaces are reported. Scattering techniques, such as SAXS, can provide a good insight into the conformation of protein chains both in solution and at interfaces.[14,15] The size distribution of droplets of both emulsions, the storage stability of the oil/water emulsions and the zeta potential (ξ) were also measured by dynamic light scattering (DLS). Images of the dried microcapsules obtained by scanning electron microscopy (SEM) are provided, with the size and morphology.

Experimental

Materials

The soy protein isolate (SPI-Supro 500E) was donated by Solae (São Paulo State, Brazil). It was dissolved in water, filtered through a 0.45 μm cellulose acetate membrane and freeze-dried prior to use. The copaiba oil was extracted from Amazon Forest Copaiba trees and kindly donated by Dr. Luiz A. Kanis (Universidade do Sul de Santa Catarina (UNISUL), Santa Catarina State, Brazil). Sodium hydroxide, acetic acid, hydrochloric acid and sodium acetate were purchased from Nuclear (São Paulo State, Brazil). The cross-linking agent 1-ethyl-3-(3-dimethylaminopropyl)-carbodiimide (EDC) was purchased from Sigma-Aldrich (USA).

Emulsion preparation

The emulsions were prepared by the following method: aqueous suspensions of SPI with the concentrations listed in Table 1 were prepared, with pH adjusted to 10 by NaOH addition. The suspensions were kept under stirring overnight, at room temperature. After this period, the pH was adjusted to 7 through HCl addition. For the samples with cross-linking agent, EDC 5% (m/m) was added at room temperature under stirring for 10 min. The suspensions were then placed in an UltraTurrax mechanical disperser (Quimis, Brazil) operated at 12,000 rpm. The copaiba oil was slowly added to the mixture, in the proportion of 0.04:1 (v/v), always under stirring.

Table 1. Composition of o/w emulsions

Sample	c_{SPI} / %, m/v	c_{EDC} / %, m/m
S1	3.0	–
S2	3.0	5.0
S3	4.0	–
S4	4.0	5.0

Emulsion size distribution and zeta potential

The mean diameter of the oil drops from the emulsions was measured on a Malvern NanoZetasizer, which uses back light scattering (at 173°) from a 4 mW He Ne laser at 632.8 nm to evaluate the size, by correlating the scattering fluctuation and using the Stokes-Einstein approximation to calculate the size from the mean diffusion coefficient. The equipment is also able to simultaneously measure the zeta potential of the sample by applying an electric potential and measuring the laser Doppler effect.

Microcapsule preparation

The resulting emulsions were kept under stirring at 12,000 rpm, and then pumped to a Spray Dryer (B-290, Büchi, Germany) in which the influx air temperature was 200 °C and outflux 70 °C, at a feeding speed of 8 mL min^{-1} and influx air speed of 35 m^3 h^{-1}. At this temperature, all the water was removed and the microcapsules were collected at the bottom of the equipment.

Imaging technique (SEM)

The morphology of the microcapsules was studied by field-emission gun scanning electron microscopy (FEG-SEM) (JEOL JSM-6701F, Japan), at a maximum amplification of 37,000 times. The samples were fixed onto metallic supports with silver glue and then sputter-coated with gold film.

Scattering techniques (SAXS and DLS)

The average size of the oil drops of the emulsions was measured through the angular dependency of the dynamic and static light scattering (DLS and SLS, respectively) using an ALV-7002 goniometer (Germany) operated with a 22 mV laser at a wavelength of 638.2 nm and able to collect data at scattering angles from 32° up to 150°. All measurements were carried out by collecting a 1.5 mL sample of each emulsion under stirring and immediately adding it to a

cylindrical glass cell without dilution. The measurements were taken immediately after that at room temperature and the data were always collected for 600 s.

The morphology of the protein chains was analyzed by SAXS at the SAX2 beam line at LNLS (Campinas-SP, Brazil), at $\lambda = 0.176$ nm and q range of $0.05 < q < 1.15$. The detection was performed with a CCD (charge-coupled device) camera with two frames of 150 s exposure and the I(q) curves were obtained after azimuthal integration of the images. The liquid samples (emulsions) were injected into a sample holder with a mica window and the solid samples were fixed with Kapton tape.

Results and Discussion

Oil/water emulsions

The size distributions of all prepared emulsions were measured immediately after preparation and after storage periods of up to ten weeks. The mean diameter of the oil drops is shown in Figure 1. As indicated in the figure, the size of the drops is close to 1 μm and varies only slightly even after 10 weeks of storage: first, an increase in size was observed, probably due to the coalescence of the oil drops, followed by a decrease, which was due to the observed creaming of larger drops, leaving only the smaller drops in suspension. Sample S4, which contained the cross-linking agent and 4% of SPI, had smaller oil drops, whereas sample S1, with less protein (3%) and without the cross-linking agent, had the largest oil drops. The obtained results also indicated that the size distributions were broad, with the polydispersity index ranging from 0.5 to 0.8.

In all cases, the zeta potential of the samples was negative and close to −50 mV, as shown in Table 2.

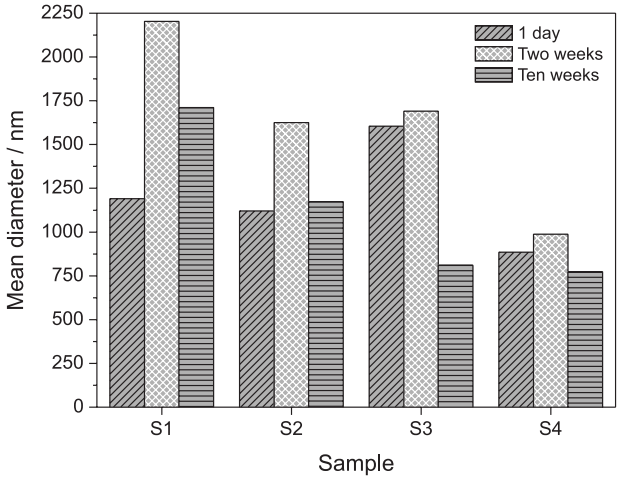

Figure 1. Mean diameter of oil drops from emulsions as a function of storage time.

The negative values for zeta potential arise from the deprotonation of carboxylic acid groups of the protein chains since the pH (7) is higher than the usual pKa values of these groups in these proteins (3.5 to 5).[15] The data also show four features: (*i*) the absolute value of the zeta potential seems to decrease with time of storage; (*ii*) this decrease is more pronounced in the samples without cross-linking agent, suggesting that some of the protein chains may leave the interface and migrate to the water phase; (*iii*) the increase in SPI concentration leads to lower absolute potential values probably due to the accompanying increase in the ionic strength of the aqueous phase; (*iv*) the absolute values for the samples with EDC are always lower than those without EDC but with the same SPI concentration. This observation might be related to the fact that after cross-linking, less acid groups are available on the protein backbone.[16]

Table 2. Zeta potential (ξ) of emulsions measured after different periods of storage

Sample	ξ / mV		
	First day	One week	Ten weeks
S1	−56.7	−49.1	−48.0
S2	−50.2	−48.0	−47.7
S3	−47.6	−45.4	−44.2
S4	−45.4	−44.0	−43.6

SPI microcapsules

All of the emulsions listed in Table 1 were spray dried in order to obtain the microcapsules. Since the mean diameter of the oil drops were observed to be dependent on the storage time, the emulsions were pumped to the spray dryer apparatus immediately after their preparation. SEM images of the dried microcapsules obtained from the emulsions are shown in Figure 2. There is a broad size distribution in which the capsule diameter ranged from 0.5 to 20 μm. The figure also shows that the surfaces of the capsules are not smooth and that some of the capsules are deflated probably due to the spray drying process.[6] Some of the images show broken capsules, in which it is possible to see that they are hollow and, therefore, these are in fact capsules and not solid spheres.

The wall thickness of the capsules is not homogeneous: the width varies from 100 to 300 nm, as shown in the FEG-SEM images in Figure 3. Some small holes in the microcapsule walls can be seen, even in the samples containing EDC. These porous structures are desirable since the intended application of these microcapsules involves the controlled-release of the inner oil phase.

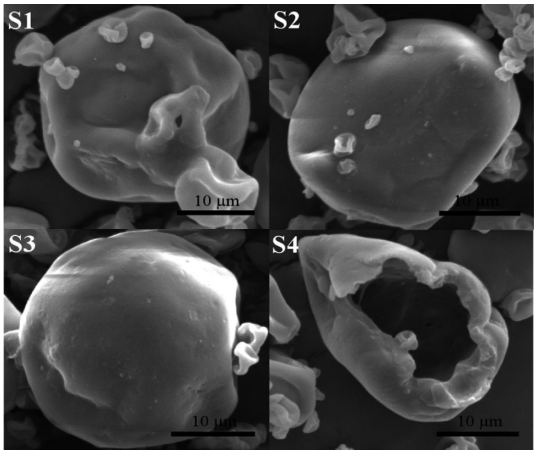

Figure 2. SEM images of microcapsules obtained from dried emulsions

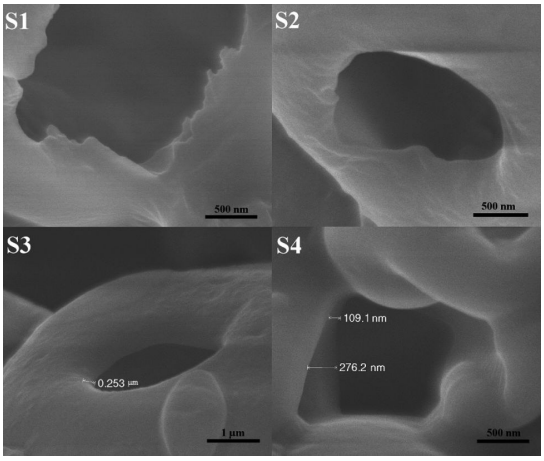

Figure 3. FEG-SEM images of microcapsules obtained from dried emulsions.

Protein at oil/water and oil/air interfaces

Since the imaging techniques provided information on the microcapsule morphology, it was possible to understand the protein chain conformations at the interfaces using these methods. However, through scattering techniques, the morphology of the SPI polymeric chains was accessed at the interface of the oil drop in water and also at the oil/air interface of the dried microcapsules.

From the angular dependency of SAXS scattering, the mean radius of gyration (R_g) of the protein chains was obtained by fitting the data at the limit $q \rightarrow 0$, according to the Guinier approximation (equation 1).[17-19]

$$\ln I = \ln I_0 - q^2\left(\frac{R_g^{\,2}}{3}\right) \quad (1)$$

The method is illustrated in Figure 4 for the SPI suspension, the emulsion S2 and microcapsules S2 and the results for all samples are summarized in Table 3.

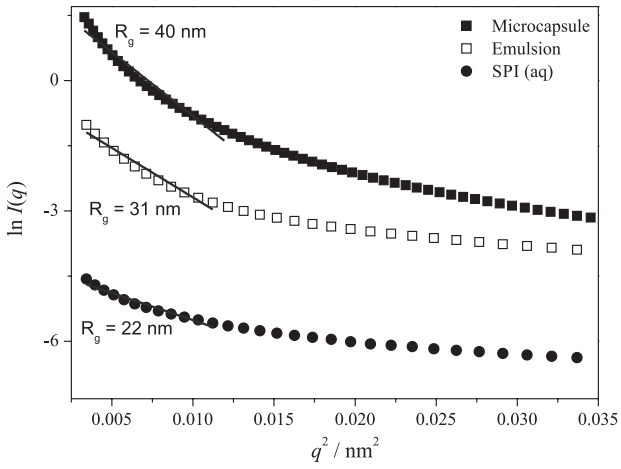

Figure 4. Guinier plot of SAXS intensity curves for the aqueous suspension of SPI, emulsion S2 and solid microcapsules prepared from emulsion S2.

Table 3. Mean radius of gyration (R_g) values obtained from the Guinier approximation of the SAXS intensity profiles for all the dispersions

Sample	R_g / nm	
	Dispersion	Microcapsule
S1	32 ± 1	40 ± 1
S2	30 ± 1	40 ± 1
S3	32 ± 1	40 ± 1
S4	31 ± 1	39 ± 1
SPI (aq)	24 ± 1	38 ± 1

As shown in Figure 4 and Table 3, the size of the SPI chains in aqueous suspension is around 24 nm. When SPI migrates to the oil-water interface, the size increases to 31 nm, indicating that the hydrophobic residues of the globular proteins are exposed to the oil phase. When the water phase is removed (dried microcapsules), the SPI chains become even larger, showing that more hydrophobic content is being exposed to the solid-air interface. In other words, the removal of water molecules from the SPI neighborhood allows the polymer chains to relax and to assume larger conformations.

Therefore, the thickness of the wall of the microcapsules (100 to 300 nm) seen in Figure 3 originates from the stacking of 4 to 12 layers of SPI. Similar values were obtained when computing the amount of SPI, the concentration of oil drops (number) and the volume fraction of the oil drops in the emulsions.

Another interesting feature observed is that in the presence of EDC (emulsions S2 and S4), the R_g values are slightly lower, indicating the contraction of the protein chains after cross-linking. The analysis of the angular dependence of the SAXS intensity is also able to show the appearance of any volume or surface fractal structure, in our case, it comprised of repetitions of SPI aggregates

at the interface. This can be achieved by fitting any linear region of the curve ln $I(q)$ *vs.* ln q, according to equation 2.[19,20] If $1 < \alpha < 3$, the linear region represents a volume fractal with a dimension $d_f = \alpha$. If the angular coefficient is $3 < \alpha < 4$, then the linear region originates from a surface fractal with dimension d_s of $6 - \alpha$.[21]

$$I(q) = I_0 q^{-\alpha} \quad (2)$$

The relationship between d_f and the topology of the scattering object can be seen in Table 4.

Table 4. Fractal dimensions of some topologies[22-26]

Topology	Fractal dimension (d_f)
Rods or linear chains	1
Random coil polymer in solution	2
Spheres with rough or fractal surface	2.5 to 3
Spheres with smooth surface	3

The SAXS data also provided some information regarding the fractal structures created by the assembly of SPI chains at the oil-water and oil-air interface. The method is exemplified in Figure 5, in which the appearance of some linear regions on the curves can be seen. Similar behaviors were observed for all other samples.

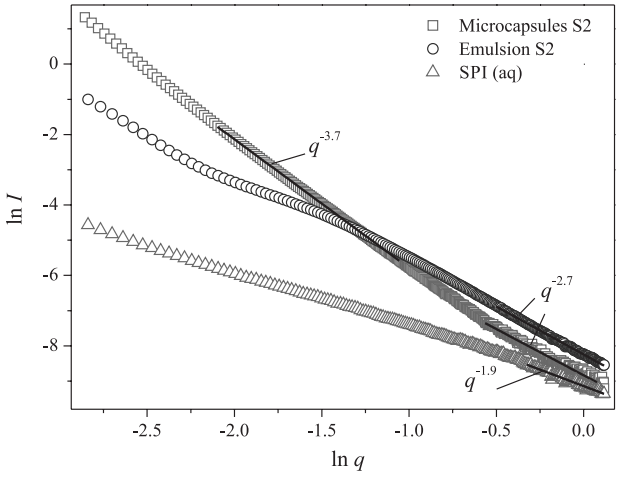

Figure 5. Double logarithmic plot of the angular dependence of the SAXS intensity for the SPI suspension and at the interface of the oil drops in the emulsion and microcapsules. The angular coefficients of the linear regions are indicated.

The small bump seen at around $q = 0.22$ nm^{-1} on the SAXS curve corresponding to the emulsion (Figure 5) originates from the structure factor of the organization of the oil drops.[27] It was observed (not shown here) that the peak disappears with the dilution of the emulsion. The process of drying the emulsions also leads to the vanishing of the structure factor peak, as seen when comparing this curve with that for the microcapsules.

The α values are given in Table 5. By comparing these values with the topologies presented in Table 4, the SPI chains assume a random coil configuration when in aqueous suspension, with a d_f value close to 1.8.; However, these chains produce a mass fractal corresponding to a sphere with a rough surface with $d_f = 2.8$ when SPI is nested at the o/w or o/air interface, which is in agreement with the information obtained from observation of the SEM images.

Table 5. α values in the SAXS $I(q)$ μ $q^{-\alpha}$ relation at high q for SPI in all dispersions

Sample	Aqueous	Dried
S1	2.74	2.69 and 3.70[a]
S2	2.80	2.96 and 3.76[a]
S3	2.83	2.67 and 3.73[a]
S4	2.58	2.96 and 3.73[a]
SPI	1.83	2.69 and 3.00[a]

[a]Lower q.

All of the curves corresponding to the dried microcapsules presented two different linear regions, at low and at high q values; the first corresponding to the surface fractal ($\alpha > 3$) and the second arising from volume fractal ($\alpha < 3$). These surface fractals with $d_s = 2.3$ only appear when SPI is nested at the microcapsule interfaces, indicating that the capsule surfaces are almost spherical. Another feature seen in Table 5 is the effect of the cross-linking agent EDC (emulsions S2 and S4); while there is no difference observed in the d_f values for emulsions with and without EDC, larger values are found for the dried samples with the cross-linking agent, in which the d_f value is almost 3, indicating increased smoothness of the surface due to the action of EDC. However, the presence of EDC does not affect the smoothness of SPI at the o/w interface, indicating that there is indeed the cross-linking of SPI, which only occurs during the spray-drying process, and is responsible for the increase in d_f.

Conclusions

The size distributions of all emulsions and dried microcapsules represented very polydisperse systems and this may be a consequence of the intrinsic polydispersity of SPI, which is in fact a mixture of several protein chains of different sizes and amphiphilic characteristics. However, even in such polydisperse systems, it was possible to observe some interesting features of SPI at the interfaces. Our results show that the biopolymer SPI can be used to

stabilize emulsions and to prepare microcapsules. The stabilization is due to the hydrophilic characteristics of the protein chains. Morphological changes were observed in the SPI chains when nested at o/w and o/air interfaces: the chains increase in size, indicating the rupture of the globular conformation of the protein promoting the exposure of the hydrophobic amino acid residues. Thus, the hydrophilic characteristics of the protein are strongly associated with its emulsifying properties.

It was also shown that a mass fractal emerges when SPI is nested at these interfaces; the fractal dimensions indicate that the surface is rougher in the absence of the cross-linking agent and becomes smoother when the chains are cross-linked during the formation of the microcapsules.

A good agreement between the SAXS results and the SEM images was observed, indicating that the microcapsule interfaces are rough.

Acknowledgments

The financial support of CNPq, the financial support from LNLS (Campinas-SP, Brazil) for the SAXS experiments, the Central Laboratory of Electron Microscopy (LCME) at UFSC for the SEM analysis and the donation of SPI from Solae (SP, Brazil) are gratefully acknowledged.

References

1. http://www.fas.usda.gov/psdonline/circulars/oilseeds.pdf, accessed in January 2013.
2. Keerati-u-rai, M.; Corredig, M.; *Food Hydrocolloids* **2009**, *23*, 2141.
3. Jong, L.; Peterson, S. C.; *Composites Part A* **2008**, *39*, 1768.
4. Walsh, D. J.; Cleary, D.; McCarthy, E.; Murphy, S.; Gerald, R. J. F.; *Food Res. Int.* **2003**, *36*, 677.
5. Rascón, M. P.; Beristain, C. I.; García, H. S.; Salgado, M. A.; *LWT -- Food Sci. Technol.* **2011**, *44*, 549.
6. Ortiz, S. E. M.; Mauri, A.; Monterrey-Quintero, E. S.; Trindade, M. A.; Santana, A. S.; Favaro-Trindade, C. S.; *LWT -- Food Sci. Technol.* **2009**, *42*, 919.
7. Favaro-Trindade, C. S.; Santana, A. S.; Monterrey-Quintero, E. S.; Trindade, M. A.; Netto, F. M.; *Food Hydrocolloids* **2010**, *24*, 336.
8. Jun-xia, X.; Hai-yan, Y.; Jian, Y.; *Food Chem.* **2011**, *125*, 1267.
9. Gan, C. Y.; Cheng, L. H.; Easa, A. M.; *Innovative Food Sci. Emerg. Technol.* **2008**, *9*, 563.
10. Mendanha, D. V.; Ortiz, S. E. M.; Favaro-Trindade, C. S.; Mauri, A.; Monterrey-Quintero, E. S.; Thomazini, M.; *Food Res. Int.* **2009**, *42*, 1099.
11. Cao, Y. M.; Chang, K. C.; *J. Food Sci.* **2002**, *67*, 1449.
12. Gomes, N. M.; Rezende, C. M.; Fontes, S. P.; Matheus, M. E.; Fernandes, P. D.; *J. Ethnopharmacol.* **2007**, *109*, 486.
13. Santos, A. O.; Ueda-Nakamura, T.; Dias Filho, B. P.; Veiga Jr., V. F.; Pinto, A. C., Nakamura, C. V.; *J. Ethnopharmacol.* **2008**, *120*, 204.
14. Spinozzi, F.; Mariani, P.; Saturni, L.; Carsughi, F.; Bernstorff, S.; Cinelli, S.; Onori, G.; *J. Phys. Chem. B* **2007**, *111*, 3822.
15. Benichou, A.; Aserin, A.; Garti, N.; *Colloids Surf., A* **2007**, *294*, 20.
16. Nakajima, N.; Ikada, Y.; *Bioconjugate Chem.* **1995**, *6*, 123.
17. Schärtl, W.; *Light Scattering from Polymer Solutions and Nanoparticle Dispersions*, vol. 1; Springer: Berlin, Germany, 2007.
18. Chu, B.; Hsiao, B. S.; *Chem. Rev.* **2001**, *101*, 1727.
19. Narsimlu, N.; Kumar, K. S.; Wuc, C. E.; Wu, C. G.; *Mater. Lett.* **2004**, *58*, 1113.
20. van-Beurten, P.; Vrij, A.; *J. Chem. Phys.* **1981**, *74*, 2744.
21. Stribeck, N.; *X-Ray Scattering of Soft Matter*, vol. 1; Springer: Berlin, Germany, 2007.
22. Sorensen, C. M.; Cai, J.; Lu, N.; *Langmuir* **1992**, *8*, 2064.
23. Sorensen, C. M.; Wang, G. M.; *Phys. Rev. E: Stat. Phys. Plasmas Fluids Relat. Interdisciplin. Top.* **1999**, *60*, 7143.
24. Lin, M. Y.; Lindsay, H. M.; Weitz, D. A.; Ball, R. C.; Klein, R.; Meakin, P.; *Proc. R. Soc. Lond., Ser. A* **1989**, *423*, 71.
25. Lin, M. Y.; Lindsay, H. M.; Weitz, D. A.; Ball, R. C.; Klein, R.; Meakin, P.; *Phys. Rev. A: At. Mol. Opt. Phys.* **1990**, *41*, 2005.
26. Hurd, A. J.; Flower, W. L.; *J. Colloid Interface Sci.* **1988**, *122*, 178.
27. Yuguchi, Y.; Thuy, T. T. T.; Urakawa, H.; Kajiwara, K.; *Food Hydrocolloids* **2002**, *16*, 515.

Submitted: February 19, 2013
Published online: May 29, 2013